Research Square

Preprints are preliminary reports that have not undergone peer review.
They should not be considered conclusive, used to inform clinical practice,
or referenced by the media as validated information.

Statistical Drivers of the Sugar-to-Ethanol Transition in Nipa Palm Sap: A Heatmap-Based Correlation of the Metabolic Pivot

Zainab Ngaini
nzainab@unimas.my
Universiti Malaysia Sarawak
Muhammad Jeffry
Universiti Malaysia Sarawak
Ana Sakura Zainal Abidin
Universiti Malaysia Sarawak
Muzamil Ayoub
Universiti Malaysia Sarawak
Kasumawati Lias
Universiti Malaysia Sarawak
Rasli Muslimen
Universiti Malaysia Sarawak
Vannessa Lawai
Universiti Malaysia Sarawak
Mohamad Sinosi
Pejabat Agama Islam Bahagian Samarahan

Article

Keywords: sugar, bioethanol, alcoholic phase, metabolic pivot, physicochemical, post-alcoholic

Posted Date: April 2nd, 2026

DOI: https://doi.org/10.21203/rs.3.rs-9165617/v1

License: This work is licensed under a Creative Commons Attribution 4.0 International License. Read Full License

Additional Declarations: No competing interests reported.

Abstract

Nipa palm sap, a sugar-rich substrate, is highly susceptible to spontaneous fermentation by environmental microbes. While anaerobic conditions are well known, the kinetics of spontaneous fermentation and subsequent acetification under atmospheric exposure remain underexplored. This study profiles ethanol yield as a function of key physicochemical parameters, including sucrose, pH, and total dissolved solids (TDS), in an oxygen-rich environment over 60 days. The ethanol concentration peaked at 4.54 ~ 10.01% on Day 4 ~ 5 before declining below 1% by Day 11 ~ 18, marking a definitive transition from the alcoholic phase to post-alcoholic activity and vinegar production onwards. The correlation analysis indicated two distinct stages (i.e., an alcoholic phase characterised by active yeast metabolism and sugar depletion, and a post-alcoholic phase driven by acetic acid bacteria). These findings provide a framework for optimising bioethanol production and sustainable bioprocessing of nipa palm resources.

1 Introduction

Nypa fruticans sap is a nutrient-dense liquid tapped from palm inflorescences, which has historically been used for beverages, sugar, and vinegar in coastal communities. Due to its high initial sugar content and a diverse native microbial load, the sap undergoes rapid spontaneous fermentation almost immediately upon collection [1,2]. While anaerobic fermentation for bioethanol is well-documented, aerobic pathways offer unique metabolic diversity and different byproduct profiles, including biomass and organic acids. Although the sap's natural conversion to vinegar through aerobic mechanisms is well documented [3] significantly less is known about the precise kinetics of fermentation under controlled aerobic circumstances.

In rural communities, sap is customarily fermented in the open-air system to yield two culturally significant products: nipa palm wine (the alcoholic stage) and nipa palm vinegar (the subsequent acetic fermentation stage) [4,5]. Beyond its role in fermented beverages, nipa palm sap is heavily used to make a sugary syrup, providing a natural alternative to conventional table sugar [6]. The versatility of nipa palm sap, including its use in the production of bioethanol and probiotic compositions, indicates a promising area for the use of bioresources [7–9]. Despite this potential, the aerobic fermentation dynamics of *Nypa fruticans* sap are largely underexplored compared to widely studied anaerobic pathways [10–12].

The spontaneous fermentation of nipa palm sap represents a significant economic liability for sugar producers. Because the sap possesses a naturally high initial sugar concentration, it is highly susceptible to the Crabtree effect, which triggers rapid spontaneous fermentation [13,14]. From a financial perspective, the conversion of sucrose into bioethanol during this initial phase causes a drastic drop in total sugar yield, thereby significantly reducing the return on investment [15]. Consistent with economic analyses of similar sugar-based commodities, the substrate sugar yield is a primary determinant of both the minimum selling price and overall profitability [16]. Consequently, spontaneous fermentation that consumes the available sugars translates directly into a proportional loss of revenue in the final sugar output.

Aerobic pathways may offer distinct advantages in terms of microbial activity and metabolite diversity, yet the current lack of comprehensive profiling limits the optimisation and scalability of these systems [17]. Specifically, monitoring ethanol concentrations daily is essential to differentiate between the intoxicating "wine" phase and the subsequent vinegar phase. This transition is characterised by a decrease in ethanol and a concurrent increase in acetic acid, driven by the metabolic activity of acetic acid bacteria (AAB). Existing research has primarily focused on short-term characterisation (typically under seven days) or has centred on anaerobic systems for bioethanol [17–19]. While some studies have explored long-term physicochemical changes alongside microbial assessments [20], There remains a significant research gap in understanding the metabolic bridge between the initial alcoholic peak and the stabilised post-alcoholic stage under aerobic conditions [5].

The precision of this metabolic profiling depends heavily on the interplay between the sap's chemical environment and its microbial succession [21,22]. For *Nypa fruticans*, which lives in mangroves, monitoring salinity is especially important, as the sap's natural salt concentration may exert selective pressure, possibly limiting spoilage organisms and favouring salt-tolerant acetic acid bacteria. Additionally, the concentration of salts and Total Dissolved Solids (TDS) that results from water evaporating in a semi-open system can change the osmotic pressure, which directly affects the rate of sugar depletion [23]. By investigating these parameters in tandem, it is possible to move beyond simple observation and begin to decipher the environmental cues that indicate the end of the alcoholic phase and the onset of stable vinegar production.

Understanding the transition from the initial alcoholic peak to the stabilised post-alcoholic stage is vital not only for process efficiency but also from a public health perspective. Consumption of the sap during an unidentified or transitional alcoholic phase can lead to unintended ethanol exposure and potential health risks [24]. Without a clear timeline of the sap's chemical transition in a slightly open container, which mimics traditional storage, consumers and producers lack the data necessary to distinguish between fresh sap, intoxicating spirits, and stable vinegar.

This study addresses these unresolved complexities by presenting a systematic profiling of ethanol and acetic acid (vinegar) concentrations, correlating these outputs with temporal shifts in physicochemical parameters, specifically pH, sucrose depletion, salinity and Total Dissolved Solids (TDS), over a 60-day aerobic incubation period. By integrating high-performance liquid chromatography (HPLC) with robust statistical analysis, this study aims to elucidate the underlying fermentation kinetics and identify critical control points within the metabolic transition. These findings provide a foundational framework for optimising fermentation strategies and enhancing shelf-life stability, which ultimately unlocks the potential of nipa palm as a sustainable feedstock for bioethanol and other high-value bioproducts.

2 Materials and Methods

2.1 Sample Collection and Fermentation Setup

Nipa palm sap was collected from four locations that were known to produce nipa palm sap products in the State of Sarawak, Malaysia. Those are Kampung Tambirat in Samarahan Division (coordinates: 1° 32' 51.0828" N, 110° 30' 44.7912" E) and Kg. Tambak, Pusa (1° 35' 38.6916" N, 111° 18' 19.998" E), Kampung Baru, Kabong (1° 49' 7.3164" N, 111° 8' 1.464" E), and Kg. Tanjong Riong, Maludam (1° 40' 32.8404" N, 111° 2' 47.1876" E) in Betong Division (see Fig. 1). Upon completion of the 24-hour collection period, the sap was transported to the laboratory for immediate processing. The fermentation trial was conducted over 60 days using 180 sterilised 50 mL centrifuge tubes (Biologix, China). Each tube contained 30 mL of freshly collected nipa palm sap. To facilitate the oxidative transition required for vinegar production, the process was maintained under aerobic conditions. The tube caps were loosely placed, and the samples were maintained undisturbed at room temperature throughout the fermentation period. Sample analysis was performed at daily intervals, with each time point analysed in triplicate (n = 3) to calculate standard errors and ensure the statistical reliability of the kinetic data.

2.2 Evaluation of Physicochemical Properties

The physicochemical characteristics of the samples of nipa palm sap were rigorously assessed during the fermentation process. The pH was measured using a calibrated pH meter (Hanna Instruments, United States), while the sucrose concentration was measured using a digital refractometer (°Brix) (Hanna Instruments, United States). TDS and water salinity were assessed using a TDS & EC meter (Yegren, China). Quantitative analysis of ethanol concentrations was performed using HPLC with a Shimadzu system (Shimadzu, Japan). Samples were centrifuged and filtered before injection into a fermentation monitoring column. All instruments were operated according to the manufacturers' protocols, and measurements were conducted in triplicate to ensure accuracy and reproducibility.

2.3 Chromatographic Analysis of Fermentation Products

Each sample was spun in a tabletop centrifuge (Daihan, South Korea) at 10,000 rpm for 10 minutes before HPLC analysis. The resulting supernatants were passed through 0.45 µm nylon syringe filters and subsequently placed into glass vials for further analysis. Ethanol and other fermentation metabolites were measured using a fermentation monitoring column (150 × 7.8 mm, Bio-Rad, Hercules, CA, USA). A 5 mM aqueous sulfuric acid (H_2SO_4) solution served as the mobile phase. A 20 µL aliquot of the sample was injected into the column, which was operated at 60°C with a flow rate of 0.8 mL/min. Detection was performed using a refractive index detector (RID-10A, Shimadzu, Kyoto, Japan) operating in positive polarity mode. The HPLC system consisted of an LC-20AT pump, a DGU-20A degasser, and a CTO-20A column oven (Shimadzu, Kyoto, Japan). Chromatographic data were collected and analysed using LC Solution software (Shimadzu, Kyoto, Japan). Calibration standards were prepared using HPLC-grade ethanol (HmbG, Malaysia) and ultrapure water (J.T. Baker, PA, USA).

2.4 Quantification of Ethanol

Ethanol was identified based on its retention time. Quantification was performed using an external calibration curve constructed from six concentration points. Calibration curves with a linearity (R^2) greater than 0.9950 were deemed acceptable for ethanol quantification. Intermediate precision was assessed using relative standard deviation (RSD), with values of 0.1% v/v for low ethanol concentration and

2.0% v/v for high ethanol concentration. The limit of detection (LOD) and limit of quantification (LOQ) were determined using the equations LOD = 3.3σ / S and LOQ = 10σ / S, where σ denotes the standard deviation of the signal response, and S refers to the slope of the calibration curve [25]. A quality control test was performed before ethanol quantification to ensure the accuracy of the calibration curve. Using the relative error method, the percentage difference between the measured peak area of ethanol at a known concentration and its actual value was calculated. Calibration curves are accepted if the relative error is within ± 5%. If the relative error exceeded the threshold, a new calibration curve is generated.

2.5 Statistical Analysis

The correlation matrix was generated using IBM SPSS Statistics software version 27.0 (Armonk, NY, USA). Calibration curve graphs and equations were drawn and calculated using Excel (Microsoft, CA, USA). A heatmap correlation matrix was generated using Python (Netherlands). Data were presented as the means ± standard deviation (SD) of three replicates. Retention times from reference standards were used to identify the peaks of the parameters of interest.

3 Results and Discussion

3.1 Sample Collection and Fermentation Setup

The schematic diagram of the sample collection and fermentation setup is shown in Fig. 2. The aerobic fermentation setup was designed for 60 days, using sterilised 50 mL centrifuge tubes as bioreactors. Although both aerobic and anaerobic environments allow wild yeasts to produce ethanol, aerobic conditions tend to generate higher levels of by products such as biomass and acetic acid [26]. This is because aerobic conditions favour cell growth and alternative metabolic pathways, which collectively reduce ethanol yield [27,28].

3.2 Visual and Physical Transitions

Daily observation of visual and physical transitions during the fermentation process showed distinct and progressive colour changes in the nipa palm sap over 60 days (Fig. 3). On Day 0, the sap was brown and transparent. By Day 4, as ethanol production peaked, the sap turned hazy and milky white, indicating active microbial fermentation [29]. Following this phase, the sap regained clarity by Day 7, accompanied by gradual browning. Due to the production of secondary metabolites from the fermentation, the sap's coloration became noticeably darker brown by Day 15, signifying a step in its chemical or physical transformation (Fig. 3d). Maillard reaction is observed during the process, as phenolic substances undergo enzymatic browning by polyphenol oxidase (PPO) and peroxidase (POD), which bacteria use to transform them into brown pigments like melanin and the interaction between remaining reducing sugars and amino acids, forming melanoidins and other Maillard reaction products which explains the browning of the sap (El Hosry et al., 2025). In the context of sap quality, this contributes to the unique flavor, aroma, and color of the sap which was reported by the locals tp have a distinct sourness, rich caramel-like flavor different than coconut vinegar. Microbial activity during fermentation alters pH and sugar levels, thereby promoting pigment development and discolouration. [30,31]. Its dynamic physicochemical character during aerobic fermentation is highlighted by this visual evolution, which is consistent with the recent investigations on nipa sap fermentation [20].

3.3 Sucrose and Ethanol Kinetics

The kinetics of sucrose depletion and ethanol accumulation are depicted in Fig. 4. Initial sucrose concentrations varied based on the sampling locations; Kabong had the highest initial sucrose at 17.7 °Brix, followed by Tambak (17.70 °Brix) and Maludam (17.67 °Brix), while Tambirat recorded the lowest at 15.43 °Brix. These variations appear closely linked to the salinity of the surrounding water sources. Kabong and Maludam, classified as mesohaline environments (10.46 ppt and 8.40 ppt), respectively, yielded higher sucrose concentrations than the oligohaline sites of Tambak and Tambirat (6.50 ppt and 2.47 ppt) (Table 1) [32,33]. This observation aligns with established theories suggesting that higher salinity induces physiological stress in Nypa fruticans, thereby stimulating increased sucrose production as an adaptive mechanism [34].

Across all four locations, sucrose degradation showed a consistent downward trajectory during the 60-day fermentation. A sharp initial reduction was observed on Day 5, with concentrations dropping by approximately half in Kabong with − 9.53 °Brix and Tambak with − 8.93 °Brix. The sharp reduction in total sugar content observed during the first 120 hr of storage corresponded with the initiation of active microbial fermentation, primarily alcoholic fermentation facilitated by indigenous yeasts such as *Saccharomyces cerevisiae* [20].

This phase corresponded to a sharp increase in ethanol concentration, peaking at Day 4–5, indicating ethanol accumulation during early fermentation of nipa palm sap under aerobic conditions [12].

On the other hand, the ethanol trend showed similarities across locations. The ethanol profile is characterised by two distinct phases: rapid alcoholic fermentation followed by a degradation stage. The exhaustion of sucrose by Day 5 marks a significant metabolic pivot, where at this juncture, the depletion of the primary substrate triggers a shift toward acetification. The sucrose depletion to its lowest point at 4.8 °Brix, (Tambirat), 5.33 (Tambak), 7.43 °Brix (Kabong), and 5.57 °Brix (Maludam), signifies a thorough analysis of substrate utilisation during 60 days of aerobic fermentation. During the alcohol fermentation, the ethanol concentration exhibited a sharp exponential increase, rising to 7.73% v/v ± 0.25 (Day 3, Tambirat), 6.74% v/v ± 0.20 (Day 3, Tambak), 8.70% v/v ± 0.230 (Day 4, Kabong), and 3.15% v/v ± 1.49 (Day 4, Maludam). These peaks continued into Day 4 for Tambirat and Tambak, reaching a maximum concentration of 7.98% ± 0.45 and 7.01% v/v ± 0.26, respectively; into Day 5 for Kabong and Maludam, reaching at 10.01% v/v ± 0.73 and 4.54% v/v ± 1.43, respectively, defining the "Golden Window" for ethanol recovery. The rapid ethanol accumulation over the 96 hours closely correlated with a significant reduction in sucrose levels and TDS, indicating a high metabolic flux. In other words, Days 4–5 mark a significant metabolic pivot, in which the exhaustion of sucrose triggers the onset of acetification. During this crucial kinetic turning point, fermentable sugar exhaustion and peak yeast activity give way to an aerobic, secondary oxidative phase in which stored ethanol is broken down to acetic acid [20]. The ethanol levels subsequently declined progressively, falling below 1% starting on Day 11 for Tambak (0.22% v/v ± 0.15) and Maludam (0.16% v/v ± 0.212), on Day 13 for Tambirat (0.67% v/v ± 0.52) and on Day 18 for Kabong (0.44% v/v ± 0.43) and remaining undetectable from Day 50 onward. The process requires nearly a month (31 days) for ethanol to be fully metabolised in an aerobic environment.

Notably, the peak in ethanol concentration coincided with the most rapid decrease in total sugar content, indicating active fermentation during this initial phase [12]. The gradual reduction in ethanol levels was attributed to volatilisation and microbial oxidation, particularly by *Acetobacter* and *Gluconobacter*, which are known to convert ethanol into acetic acid under aerobic conditions [35]. This metabolic shift was supported by the concurrent stabilisation of sugar levels and the decline in ethanol concentration after Day 13.

The sugar depletion and ethanol production pattern also suggested a dynamic microbial succession. Early dominance by fermentative yeasts was likely followed by lactic acid and acetic acid bacteria [14,20]. This succession not only altered the chemical composition but also affected the sensory and nutritional quality of the sap, rendering it unsuitable for direct consumption or sugar production beyond the initial days. Moreover, the peak ethanol yield observed in this study (4.54–10.01 % v/) is comparable to those reported for optimised open-vessel fermentation systems that permit acetic acid production [12].

Furthermore, the alcoholic fermentation process continues even in the presence of oxygen, whereas standard alcoholic fermentation typically requires a strictly anaerobic environment. The high initial sucrose concentration in the nipa palm sap triggers the Crabtree effect, enabling the onset of alcoholic fermentation [36]. This phenomenon facilitates ethanol production under less stringent conditions, such as in loosely sealed vessels, thus creating an economic opportunity for the tapper to produce bioethanol. Nevertheless, the window for optimal production is time-restricted as the ethanol titer peaks between Days 4 and 5, marking the ideal time for harvesting. After Day 5, ethanol levels begin to decline, thereby reducing overall yield.

Because fermentation persists even under aerobic conditions due to the Crabtree effect, sugar quality decreases drastically, with sucrose concentration halving by Days 4 to 5. Consequently, the production of sugar products, such as sugar syrup (*Gula Apong*), must commence on Day 0. By Day 1, the sap already exhibits a concentration loss of 0.6 to 1.13 °Brix, indicating that the degradation of sap sugar concentration occurs almost immediately. Therefore, to maximise the yield of sugar derived from nipa palm sap, processing must be initiated on Day 0 to preserve the initially high sugar concentration.

The fermentation kinetics suggest a metabolic pivot occurred at Day 4–5, where the primary metabolism transitions from alcoholic fermentation to ethanol oxidation. This is evidenced by the ethanol concentration reaching 4.54–10.01% v/v while sucrose levels drop to 9.00–13.50 °Brix. Beyond this point, even in the presence of residual sugar, the aerobic environment facilitates a switch in carbon source utilisation from sucrose to ethanol [35] .

Table 1
Initial sucrose content of nipa palm sap and salinity of water sources near the sampling sites.

Sampling Locations	Initial Sucrose Concentration (°Brix)	Water Salinity (ppt)	Classification
Tambirat	15.43	2.47	Oligohaline
Tambak	17.70	6.50	
Maludam	17.67	8.40	Mesohaline
Kabong	19.50	10.46	

Figure 5 illustrates the scatter plot of comparative analysis of sucrose (°Brix) and peak intensities of total sugars measured by HPLC. The linear regression indicates a strong git (R^2 = 0.800). Furthermore, a Pearson correlation test verified that the sugar peaks and °Brix readings are normally distributed and share a strong, positive, and statistically significant relationship (r = 0.895, p < 0.001). Detailed results are available in **Supplementary Figure S1 and Tables S1, S2, and S3**. In parallel, total sugar content was also monitored using a refractometer, which estimates sucrose concentration in °Brix by measuring the refractive index. This approach provides a comparative evaluation of dissolved sugars in plant sap, expressed as sucrose equivalent[37]. A comparable trend was observed across both measurement techniques, indicating consistent detection of sucrose and total sugar concentrations. A pronounced decline in sucrose levels between Day 0 and Day 3 corresponded to the drop in sugar peak heights. Beyond Day 3, both parameters continued to decrease gradually, reflecting a consistent trend in their physicochemical changes. A similar study demonstrating a linear relationship between refractometer Brix readings and HPLC-determined total sugar concentration has previously been reported, in which the total °Brix value measured by a refractometer was equivalent to 0.96 of the total sugars determined by HPLC, indicating a strong linear correlation. This is due to the direct proportionality between the refractive index and the sugar concentration in the sap, which enables °Brix measurements to accurately reflect the actual sugar content [38].

3.3.1 Ethanol Quantification via HPLC

Ethanol concentration was quantitatively determined using HPLC. The chromatograms of ethanol standards, fermented nipa palm sap samples and a calibration curve are available in **Supplementary Figure S2**. The ethanol peaks were consistently observed at 8.7 minutes, which closely matched the standard's retention time. The chromatographic baseline remained stable throughout the analysis, demonstrating the reliability and suitability of the HPLC settings for daily monitoring of fermentation products [25,39]. The calibration curve demonstrates excellent linearity with an R^2 value of 1. The method exhibited a limit of detection (LOD) of 0.01% and a limit of quantification (LOQ) of 0.03%, confirming its high sensitivity and suitability for ethanol analysis.

3.3.2 Method Validation

Method validation was conducted to determine the linearity, precision, LOD and LOQ of the calibration curves **(**Table 2**).** The calibration curves exhibited strong linearity with correlation coefficients (R^2) approaching 1.0000, indicating high accuracy and reliability in quantifying ethanol concentrations. Throughout the 60-day analytical period, calibration curve equations were updated at variable intervals, ranging from daily adjustments to weekly recalibrations, based on instrumental stability and standard response behaviour with a coefficient of determination (R^2) exceeding 0.995 [40]. The calibration curve for higher ethanol concentrations yielded an R^2 value of 0.9986, which exceeds the commonly accepted threshold of 0.9950, indicating excellent linearity and reliability of the measurement [41]. The precision of the ethanol calibration curves for both low and high concentrations, expressed as coefficients of variation, was 3.21% and 2.09%, respectively. The calibration curve equations are available in **Supplementary Table S4 and Table S5**. These values fall well below the maximum permissible limit of 5%, thereby confirming the reliability and precision of the analytical method [42]. All calibration curves used to quantify ethanol concentration passed quality control, with relative errors below 5%. These parameters were specifically computed for lower concentrations of ethanol to evaluate the sensitivity of the analytical method in detecting and quantifying trace levels. The methodology confirms the suitability of this approach for routine fermentation analysis [25].

Table 2
Validation parameters based on concentration.

Parameters	Concentration (% v/v)	Linear calibration curve	Linearity (R^2)	Precision %	LOD (% v/v)	LOQ (% v/v)
Ethanol (Low)	0.10-2.0	y= (399880 ± 114042)x + (8174 ± 14527)	0.9980 ± 0.0019	3.21	0.07 ± 0.09	0.24 ± 0.30
Ethanol (High)	1.0–10.0	y= (397816 ± 101711)x + (22758 ± 18077)	0.9986 ± 0.0014	2.09	0.21 ± 0.11	0.69 ± 0.37

3.4 pH and TDS Dynamics

Figure 6 illustrates the pH value and TDS during 60 days of nipa palm sap fermentation. The initial pH for all sampling locations were different, where Kabong was the most neutral at pH 6.38 followed by Maludam (5.91), Tambak (5.85) and Tambirat which was the most acidic at 5.56 The pH dropped significantly to 3.90–4.70 (Day 1) and continued to a minimum in the range of 3.30–3.80. After Day 20, the pH remained stable with slight fluctuation until the end of Day 60. After this point, the pH rose slightly to 360–4.20 by Day 60. This results from overoxidation, which dilutes the acid content by further oxidising acetic acid into water[43 44].

A pronounced increase in TDS was observed for all four sampling locations from Day 0 (1900–2200 ppm) to Day 1 (2200–3200 ppm), reflecting microbial biomass accumulation [45]. This was followed by a gradual upward trend, with TDS values stabilising between 3500–3800 ppm and 4200–4300 ppm from Day 10 to Day 60, respectively. Small variations were noted during the fermentation process, with a significant decrease on Day 42 for Tambirat (3752 ppm ± 0) that might be the result of temporary microbial stress or changes in metabolic activity. The overall increase in TDS suggests a steady buildup of soluble compounds, including yeast biomass, microbial and cell reproduction, and trace amounts of pectin, amino acids, and organic acids generated during the fermentation process [46,47]. This pattern indicates continuous metabolic changesn the fermentation medium [48]. This suggests the 60-day mark is the point of chemical equilibrium for the aerobic fermentation of nipa sap.

3.7 Correlation Analysis of the physicochemical parameters

Figure 7 **and** Fig. 8 show the statistical drivers of the alcoholic and post-alcoholic heatmap-based correlation analysis among key physicochemical parameters, namely ethanol, sugars, pH, and TDS during both the alcoholic and post-alcoholic fermentation stages. The analysis highlights the dynamic interrelationships between these variables throughout the fermentation process. The correlation matrix reveals distinct patterns and associations that characterise each stage, offering insights into the underlying biochemical mechanisms. Detailed correlation data are provided in **Supplementary Tables S1, S6 and S7.**

3.7.1 Alcoholic Fermentation Stage (Day 0 to Day 4–5)

The alcoholic fermentation phase under aerobic conditions is shown in Fig. 7a. Ethanol showed a near-perfect negative correlation with sucrose (r = − 0.934), signifying active glucose consumption and indicating a direct stoichiometric conversion. This metabolic pattern is consistent with the Crabtree effect (Fig. 7b), wherein *S. cerevisiae* preferentially undergoes fermentation rather than respiration in the presence of high sugar concentrations, even when oxygen is available [49,50]. This causes rapid glucose consumption and the ethanol spike observed in the data. Thus, this strong negative correlation statistically confirms the Crabtree effect as *S. cerevisiae* bypassing respiration to favour fermentation due to the high initial sugar concentration, despite the presence of oxygen. Not only that, the strong correlation value suggests that the depletion of sucrose is almost exclusively driving ethanol synthesis in this phase.

A positive correlation with TDS (r = 0.895) statistically confirms rapid biomass production of microbial cell growth during alcohol synthesis, which increases solute concentration in the medium [41]. Simultaneously, a negative correlation between ethanol and pH (r = − 0.597) suggests that ethanol production is associated with medium acidification. This phenomenon was due to the generation of organic acids, including minor amounts of acetic acid, during glucose metabolism, leading to a decline in the sample's pH [51,52]. Conversely, the negative correlation between sucrose and TDS (r = -0.929) highlighted that sucrose is concomitant with the increase of microbial biomass, which leads to an increase in TDS [53] The positive correlation between sucrose and pH (r = 0.691) demonstrates that

the depletion of sugars by fermenting microorganisms is associated with a decrease in pH due to the ongoing production of acidic metabolites under these aerobic conditions [52] Hence, it corresponds to the negative correlation between pH and TDS (r = -0.788), reinforcing the relationship between acidification and solute accumulation during aerobic fermentation [47].

3.7.2 Post-Alcoholic Fermentation Stage (Day 4–5 to 60)

The correlation matrix for the post-alcoholic fermentation stage from Day 4 onwards (as shown in Fig. 8) reveals significant insights into the interrelationships among key physicochemical parameters. A weak correlation between ethanol and pH suggests a non-linear or indirect relationship. This phenomenon implies that while these parameters may not be tightly coupled, they may still interact within the complex biochemical dynamics of post-alcoholic fermentation.

Ethanol and sucrose displayed a moderate positive correlation (r = 0.376), as acetic acid bacteria concurrently depleted both. This phenomenon is attributed to the metabolic activity of acetic acid bacteria (AAB), which utilise ethanol as a substrate for acetic acid production and are capable of oxidising glucose to gluconic acid [35]. Furthermore, the moderate correlation was due to the rate at which ethanol oxidation and sugar depletion happen at different speeds as sap transitions into the post-alcoholic phase. A strong negative correlation between ethanol and TDS (r = -0.587) indicates that biomass continues to accumulate even as ethanol is consumed. This observation supports the hypothesis of a secondary fermentation phase, during which AAB and other microorganisms contribute to increased TDS by accumulating biomass and metabolising acetic acid [54]. The negative correlation between sucrose and pH (r = -0.543) further substantiates the notion of sustained microbial activity, as glucose oxidation continues to drive gluconic acid production, thereby lowering the pH. Temporal analysis indicates two distinct phases: from Day 6 to Day 18, a declining pH trend corresponds with active acetic acid fermentation. Beyond Day 18, a slight increase in pH despite continued glucose depletion suggests a transition to an overoxidation phase [55]. During this phase, the produced acetic acid may be further oxidised to water and carbon dioxide, diluting the medium and raising the pH [56,57].

The metabolic shift was further supported by the different correlation profiles between the two fermentation stages. In the alcoholic stage (Days 0 to 4–5), ethanol production is strictly driven by sucrose depletion (correlation = -0.934) (Fig. 7). The connection reversed after the transition into the post-alcoholic stage; ethanol started to degrade and showed a high negative correlation (r = -0.587) with TDS, which increased further to 4200–4300 ppm by Day 60 (Fig. 6). This suggests that ethanol itself becomes a substrate for the production of non-volatile metabolites [35]. The negative correlation between sucrose and TDS (r = -0.736) reinforces the role of non-yeast microbial activity in biomass production, particularly through AAB metabolism, which utilises both glucose and acetic acid [55]. The weak correlation between pH and TDS (r = 0.380) indicates that these parameters are not directly interdependent.

The overall chemical process involves two stages of fermentation: alcoholic fermentation and post-alcoholic fermentation. The alcoholic fermentation (Scheme 1a**)** involves yeast converting sugars into ethanol and carbon dioxide. Whereas the post-alcoholic fermentation stages (Scheme 1b) involve AAB converting ethanol into acetic acid and glucose into gluconic acid.

3.7.3 Principal Component Analysis of the Fermentation Trends

Figure 9 shows the scatter plot of the principal component analysis of the fermentation trends. The overall fermentation trends were not influenced by the sampling locations (Fig. 9a) or water salinity (Fig. 9c). The data points for Tambirat, Tambak, Kabong, and Maludam overlap heavily and do not form distinct, isolated clusters. This indicates that the geographical origin of the sap does not significantly alter the overall trend of the fermentation process; thus, the fundamental physicochemical changes occurring during fermentation are consistent across all four sampling sites. Similar to the location plot, the points for Mesohaline and Oligohaline water types are thoroughly intermixed. Thus, this supports that water salinity does not influence the overall fermentation trend. Despite the initial sucrose concentration being affected by the water salinity (Table 1), its influence diminishes as the fermentation kinetics take over, leading to a uniform process overall [34]. Hence, this explains the similarity in the fermentation trend of nipa palm sap fermentation under aerobic conditions in other place such as in the Philippines [12].

Unlike location and salinity, the fermentation phase shows a clear pattern of dispersion and clustering (Fig. 9b). The alcohol phase exhibits a wide spread across both axes. In contrast, the post-alcoholic phase, including depleted alcohol, forms a much tighter, more concentrated cluster in the lower-left quadrant. The wide variance during the alcohol phase reflects the highly dynamic nature of active fermentation, in which substrates such as sucrose are rapidly converted into ethanol. Whereas the tight clustering of the post-alcohol phase suggests that once the active alcoholic fermentation ceases, the physicochemical profile of the samples stabilises and becomes highly uniform, regardless of the origin of the saps.

Therefore, the fermentation trends of nipa palm sap were not influenced by geographical factors and water salinity. While the fermentation phases show a high degree of dynamic behaviour, the alcohol fermentation phase became uniform and stable, and the chemical profile during the post-alcoholic phase began.

4 Conclusion

The aerobic fermentation of *Nypa fruticans* sap follows a distinct kinetic path, with ethanol yield peaking at 7.98% on Day 4. The 60-day observation period shows that although the "Golden Window" for ethanol is reached on Day 4, the oxidative transition that follows produces a vinegar product that is chemically stable and retains its physicochemical integrity until Day 60. This study establishes pH and TDS as trustworthy proxy indicators for real-time fermentation monitoring by comparing them with HPLC-verified metabolite profiles. The transition to a post-alcoholic phase marked by acetic acid metabolism and subsequent overoxidation was clearly captured through 60 days of monitoring. Salinity affects the initial sugar concentration of the sap, and correlation reveals a uniform trend of fermentation throughout different salinity Finally, based on precise kinetic thresholds, these results offer a strategic roadmap for the Nipa palm biorefineries model to produce bioethanol early in the cycle and transitions to vinegar while optimising resource efficiency, product shelf life and minimising waste.

Declarations

Acknowledgements

The authors wish to express their gratitude to the Jabatan Mufti Negeri Sarawak for the financial support.

Author Contributions

All authors contributed to the conception and design. Zainab Ngaini, Muhammad Jeffry, Ana Sakura Zainal Abidin and Muzamil Ayoub performed material preparation, data collection, and analysis. Muhammad Jeffry and Muzamil Ayoub conducted the laboratory analysis; Zainab Ngaini, Muhammad Jeffry and Ana Sakura Zainal Abidin prepared the manuscript; Kasumawati Lias, Mohamad Sinosi, Rasli Muslimen and Vannessa Lawai proofread and approved the final manuscript.

Data Availability Statement

The authors declare that the data supporting the findings of this study are available within the manuscript and the supplementary files.

Research Funding

This research did receive funding from the Jabatan Mufti Negeri Sarawak (Grant ID: IRG/F07/JMNS/86658/2025).

Ethics approval and consent to participate

Not applicable

Consent for publication

Not applicable

References

1. Limtong, S., Am-In, S., Kaewwichian, R., Kaewkrajay, C. & Jindamorakot, S. Exploration of yeast communities in fresh coconut, palmyra, and nipa palm saps and ethanol-fermenting ability of isolated yeasts. *Antonie Van Leeuwenhoek* **113**, 2077–2095 (2020).
2. Athirah, D. N., Asaruddin, M. R., Bhawani, S. A., Simbas, A. F. & Jack, K. S. Effect of preservative and preservation methods on physical, chemical and microbiological properties of nipa palm (Nypa fructicans) sap. *BMC Res. Notes* **18**, 136 (2025).
3. Bhat, S. V., Akhtar, R. & Amin, T. An Overview on the Biological Production of Vinegar. *Int. J. Fermented Foods* **3**, 139 (2014).
4. Macapagal Quinto, K. M. Exploring the Practices in the Traditional Nipa Vinegar Production in Lingayen Pangasinan. *IRE Journals* **7**, (2024).
5. Perral, C., Adlaon, M., Andrea Moleta Perral, C. & Agron Agri R, I. J. Analysis of Sap and liquor from Nipa (Nypa fruticans Wurmb.) fruit stalk using adopted nipa sap closed collection vessel in Barangay Ipil and Barangay Villafranca, Gigaquit, Surigao del Norte

Perral and Adlaon. *Int. J. Agron. Agri. R* http://www.innspub.net (2024).

6. Hafsanjani Salleh, M. *et al.* Proximate, Chemical and Minerals Characterization of Nypa fruticans Palm Sugar Produced by Reverse Osmosis-Pan Boiling (RO-PB) Method. *Borneo Journal of Sciences and Technology* **6**, (2024).
7. Jara'ee, J., Awg-Adeni, D. S., Bilung, L. M. & Azmin, P. Effects of selected preservation techniques on the shelf-life of nipa sap. *Food Res.* **9**, 40–48 (2025).
8. Borah, M., Mandal, M. & Konwar, B. K. Characterization of probiotic strains of Bacillus sp. from fermented palm wine (Nypa fructicans sp.) and exploration of cellulolytic potential for use as an addition in animal feed. *International Microbiology* **28**, 965–977 (2024).
9. Tamunaidu, P., Matsui, N., Okimori, Y. & Saka, S. Nipa (Nypa fruticans) sap as a potential feedstock for ethanol production. *Biomass Bioenergy* **52**, 96–102 (2013).
10. Saithong, P., Nitipan, S. & Permpool, J. Optimization of vinegar production from nipa (Nypa fruticans Wurmb.) sap using surface culture fermentation process. *Applied Food Biotechnology* **6**, 193–200 (2019).
11. Madigal, J. P. T. Assessment of the Physico-chemico and Microbiological changes during Nipa (Nypa fruticans) Sap Fermentation collected from different sites in Cagayan province, Philippines. *Indian J. Sci. Technol.* **13**, 3230–3236 (2020).
12. Manzano, L. F. T., Halabaso, E. R., Aglipay, L. R., Gamboa, F. A. & Agrupis, S. C. Evaluation of the Physico-chemical and Biological Properties of Fermented Nipa (Nypa fruticans) Sap Under Closed and Open Vessel Fermentation System for Bioethanol Production. *Open Biotechnol. J.* **18**, (2024).
13. Alcántara-Hernández, R. J. *et al.* The bacterial community in 'taberna' a traditional beverage of Southern Mexico. *Lett. Appl. Microbiol.* **51**, 558–563 (2010).
14. Ansar, Nazaruddin, Azis, A. D. & Fudholi, A. Tapping into Palm Sap: Insights into extraction practices, quality profiles, fermentation chemistry, and preservation techniques. *Heliyon* **10**, e35611 (2024).
15. Ajala, E. O., Ighalo, J. O., Ajala, M. A., Adeniyi, A. G. & Ayanshola, A. M. Sugarcane bagasse: a biomass sufficiently applied for improving global energy, environment and economic sustainability. *Bioresources and Bioprocessing 2021 8:1* **8**, 87- (2021).
16. Abedi, E. & Hashemi, S. M. B. Efficient production of lactic acid from cellulose and xylan in sugarcane bagasse by newly isolated Lactiplantibacillus plantarum and Levilactobacillus brevis through simultaneous saccharification and co-fermentation process. *Heliyon* **9**, e17935 (2023).
17. Tamunaidu, P., Kakihira, T., Miyasaka, H. & Saka, S. Prospect of Nipa Sap for Bioethanol Production. in *Green Energy and Technology* vol. 66 159–164 (Springer, Tokyo, 2011).
18. Chairul, Evelyn, Syaiful, B. & Ella, A. A Novel Immobilization Method of Saccharomyces cerevisiae on Fermentation of Nipa Palm Sap for Fuel Grade Bioethanol Production. *Key Eng. Mater.* **849**, 53–57 (2020).
19. Prasetyo, C. P., Effendi, A. J. & Chaerul, M. Analysis of the potential and characteristics of Nipa (Nypa fruticans) as a sustainable biofuel alternative source in Indonesia. *E3S Web of Conferences* **485**, 03001 (2024).
20. Jaraee, J., Adeni, A., Bilung, D. S. & Azmin, L. M. Physicochemical and microbiological assessment of Nypa fruticans sap collected in Sarawak, Malaysia. *Food Res.* **6**, 44–50 (2023).
21. Kim, N. *et al.* Soil assessment after chemical accidents using metabolic profiling and microbial community evaluation. *Chemosphere* **268**, 129362 (2021).
22. Othibeng, K. *et al.* Metabolic Circuits in Sap Extracts Reflect the Effects of a Microbial Biostimulant on Maize Metabolism under Drought Conditions. *Plants* **11**, 510 (2022).
23. Passman, F. J. Biodeterioration. *Fuels and Lubricants Handbook: Technology, Properties, Performance, and Testing, 2nd Edition* 1231–1273 (2018) doi:10.1520/mnl37-2nd-eb.
24. Dasgupta, A. Alcohol a double-edged sword. in *Alcohol, Drugs, Genes and the Clinical Laboratory* 1–21 (Elsevier, 2017). doi:10.1016/B978-0-12-805455-0.00001-4.
25. ICH. Validation of Analytical Procedures Q2(R2). (2023).
26. Duncan, J. D., Devillers, H., Camarasa, C., Setati, M. E. & Divol, B. Oxygen alters redox cofactor dynamics and induces metabolic shifts in Saccharomyces cerevisiae during alcoholic fermentation. *Food Microbiol.* **124**, 104624 (2024).
27. Tronchoni, J., Gonzalez, R., Guindal, A. M., Calleja, E. & Morales, P. Exploring the suitability of Saccharomyces cerevisiae strains for winemaking under aerobic conditions. *Food Microbiol.* **101**, 103893 (2022).

28. Veras, H. C. T., Parachin, N. S. & Almeida, J. R. M. Comparative assessment of fermentative capacity of different xylose-consuming yeasts. *Microb. Cell Fact.* **16**, 153 (2017).
29. Radi, N. A., Abu Bakar, F. & Mat Hashim, D. Determination of volatile compounds in fresh and fermented nipa sap (Nypa fruticans) using static headspace gas chromatography-mass spectrometry (GC-MS). http://www.ifrj.upm.edu.my/20%20%2801%29%202013/51%20IFRJ%2020%20%2801%29%202013%20Fatimah%20%28108%29.pdf (2013).
30. Singh, B. *et al.* Pardeamiento enzimático de frutas y verduras: una revisión. *Enzymes in Food Technology: Improvements and Innovations* 63–78 (2018).
31. Gupta, K. *et al.* Microbial Fermentation: Basic Fundamentals and Its Dynamic Prospect in Various Industrial Applications. *Industrial Microbiology and Biotechnology* 107–128 (2022) doi:10.1007/978-981-16-5214-1_4.
32. Zhu, Z. Y. *et al.* The nonconservative distribution pattern of organic matter in the Rajang, a tropical river with peatland in its estuary. *Biogeosciences* **17**, 2473–2485 (2020).
33. Antonov, J. I. & Levitus, S. World ocean atlas 2005. Vol. 2, Salinity. Preprint at http://repository.library.noaa.gov/view/noaa/1127 (2006).
34. Saelee, N. Effects of soil salinity on nutritional compositions of fresh Jak (Nypa fruticans) sap. *Journal of Food Composition and Analysis* **114**, 104767 (2022).
35. Guillamón, J. M. & Mas, A. Acetic Acid Bacteria. in *Molecular Wine Microbiology* 227–255 (Elsevier, 2011). doi:10.1016/B978-0-12-375021-1.10009-8.
36. Hagman, A., Säll, T. & Piškur, J. Analysis of the yeast short-term Crabtree effect and its origin. *FEBS J.* **281**, 4805 (2014).
37. Jaywant, S. A., Singh, H. & Arif, K. M. Sensors and Instruments for Brix Measurement: A Review. *Sensors* **22**, 2290 (2022).
38. Tamunaidu, P. & Saka, S. On-site sugar analysis and pre-treatment of Nipa Saps. *Green Energy and Technology* **108**, 121–126 (2012).
39. Snyder, L. R., Kirkland, J. J. & Dolan, J. W. *Introduction to Modern Liquid Chromatography*. *Introduction to Modern Liquid Chromatography* (Wiley, 2009). doi:10.1002/9780470508183.
40. Konieczka, P. The Role of and the Place of Method Validation in the Quality Assurance and Quality Control (QA/QC) System. *Crit. Rev. Anal. Chem.* **37**, 173–190 (2007).
41. Zhao, X., Mu, Y. & Yang, M. A simple multi-residue method for determination of plant growth retardants in Ophiopogon japonicus and soil using ultra-performance liquid chromatography–tandem mass spectrometry. *Chemosphere* **207**, 329–336 (2018).
42. Gao, Y., Ierapetritou, M. G. & Muzzio, F. J. Determination of the Confidence Interval of the Relative Standard Deviation Using Convolution. *J. Pharm. Innov.* **8**, 72–82 (2013).
43. Gomes, R. J., Borges, M. de F., Rosa, M. de F., Castro-Gómez, R. J. H. & Spinosa, W. A. Acetic Acid Bacteria in the Food Industry: Systematics, Characteristics and Applications. *Food Technol. Biotechnol.* **56**, 139 (2018).
44. Głąb, S. & Hulanicki, A. pH. in *Encyclopedia of Analytical Science* 72–78 (Elsevier, 2005). doi:10.1016/B0-12-369397-7/00445-3.
45. Vieira, É. D., Andrietta, M. da G. S. & Andrietta, S. R. Yeast biomass production: a new approach in glucose-limited feeding strategy. *Brazilian Journal of Microbiology* **44**, 551–558 (2013).
46. Beng Lee, B., . H. J. T. & . E. S. C. Fed-batch Fermentation of Lactic Acid Bacteria to Improve Biomass Production: A Theoretical Approach. *Journal of Applied Sciences* **7**, 2211–2215 (2007).
47. Thuy, C. X. *et al.* Effect of Fermentation Conditions (Dilution Ratio, Medium pH, Total Soluble Solids, and Saccharomyces cerevisiae Yeast Ratio) on the Ability to Ferment Cider from Tamarillo (Solanum betaceum) Fruit. *J. Food Process. Preserv.* **2024**, 1–17 (2024).
48. Abidin, A. S. Z. *et al.* Physicochemical Investigation and Analysis of Nypa Sap (Nypa fruticans Wurmb) using a Novel Collecting Device. *Borneo Journal of Resource Science and Technology* **14**, 54–68 (2024).
49. Pfeiffer, T. & Morley, A. An evolutionary perspective on the Crabtree effect. *Front. Mol. Biosci.* **1**, 17 (2014).
50. Maicas, S. The Role of Yeasts in Fermentation Processes. *Microorganisms* **8**, 1142 (2020).
51. Porro, D. & Branduardi, P. Production of Organic Acids by Yeasts and Filamentous Fungi. in *Biotechnology of Yeasts and Filamentous Fungi* 205–223 (Springer International Publishing, Cham, 2017). doi:10.1007/978-3-319-58829-2_7.
52. Coote, N. & Kirsop, B. H. Factors Responsible for the Decrease in pH during Beer Fermentations. *Journal of the Institute of Brewing* **82**, 149–153 (1976).
53. Lips, D. Fuelling the future of sustainable sugar fermentation across generations. *Engineering Biology* **6**, 3–16 (2022).

54. Zheng, Y. *et al.* Kinetics of predominant microorganisms in the multi-microorganism solid-state fermentation of cereal vinegar. *LWT* **159**, 113209 (2022).
55. Mamlouk, D. & Gullo, M. Acetic Acid Bacteria: Physiology and Carbon Sources Oxidation. *Indian J. Microbiol.* **53**, 377 (2013).
56. He, Y. *et al.* Oxidative Fermentation of Acetic Acid Bacteria and Its Products. *Front. Microbiol.* **13**, 879246 (2022).
57. Saeki, A., Taniguchi, M., Matsushita, K., Toyama, H. & Theeragool, G. Microbiological Aspects of Acetate Oxidation by Acetic Acid Bacteria, Unfavorable Phenomena in Vinegar Fermentation. *Biotechnology, and Biochemistry* **61**, 317–323 (1997).

Scheme 1

Scheme 1 is available in the Supplementary Files section.

Figures

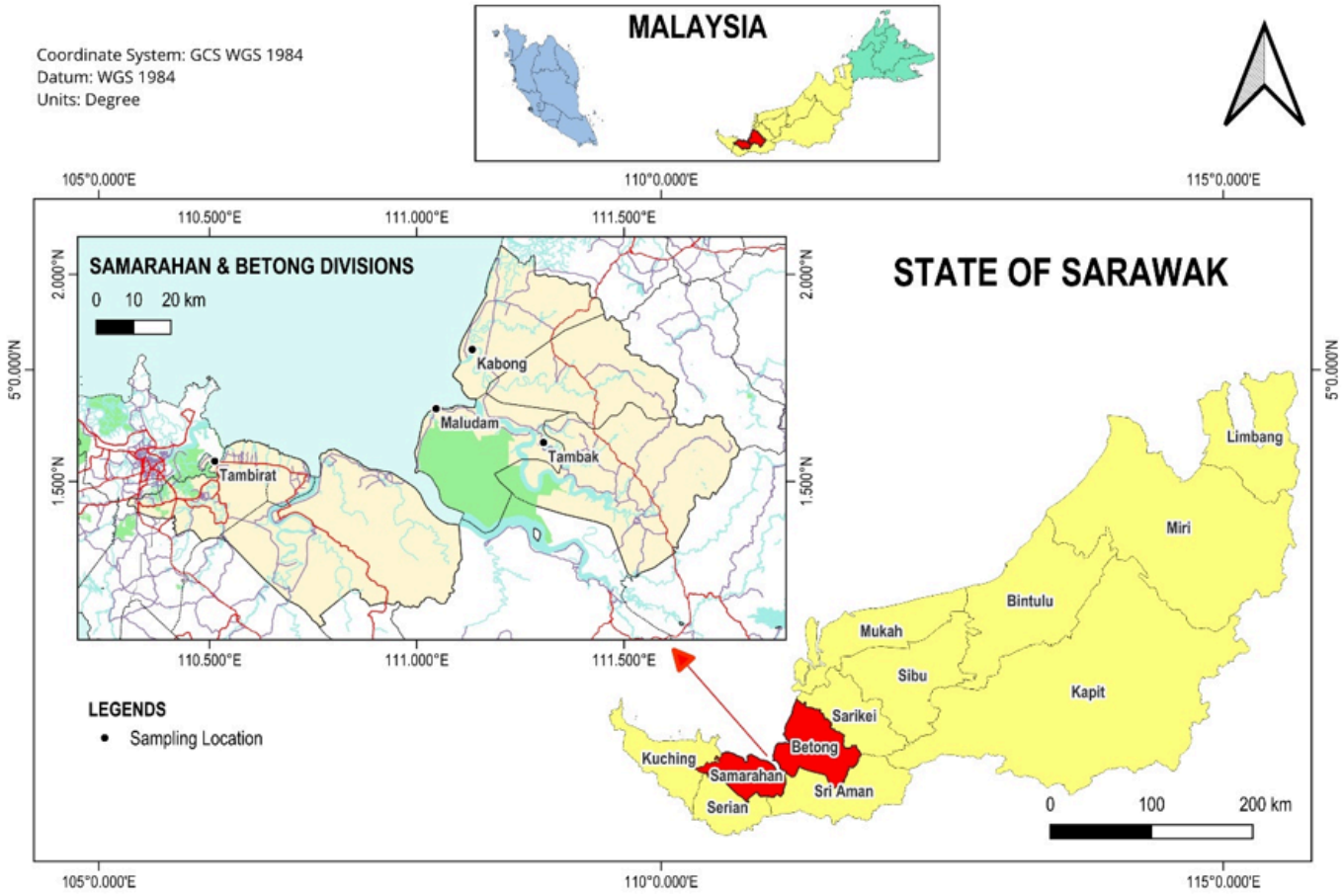


Figure 1

Map of sampling locations for nipa palm sap in the Samarahan and Betong Divisions, Sarawak, Malaysia.

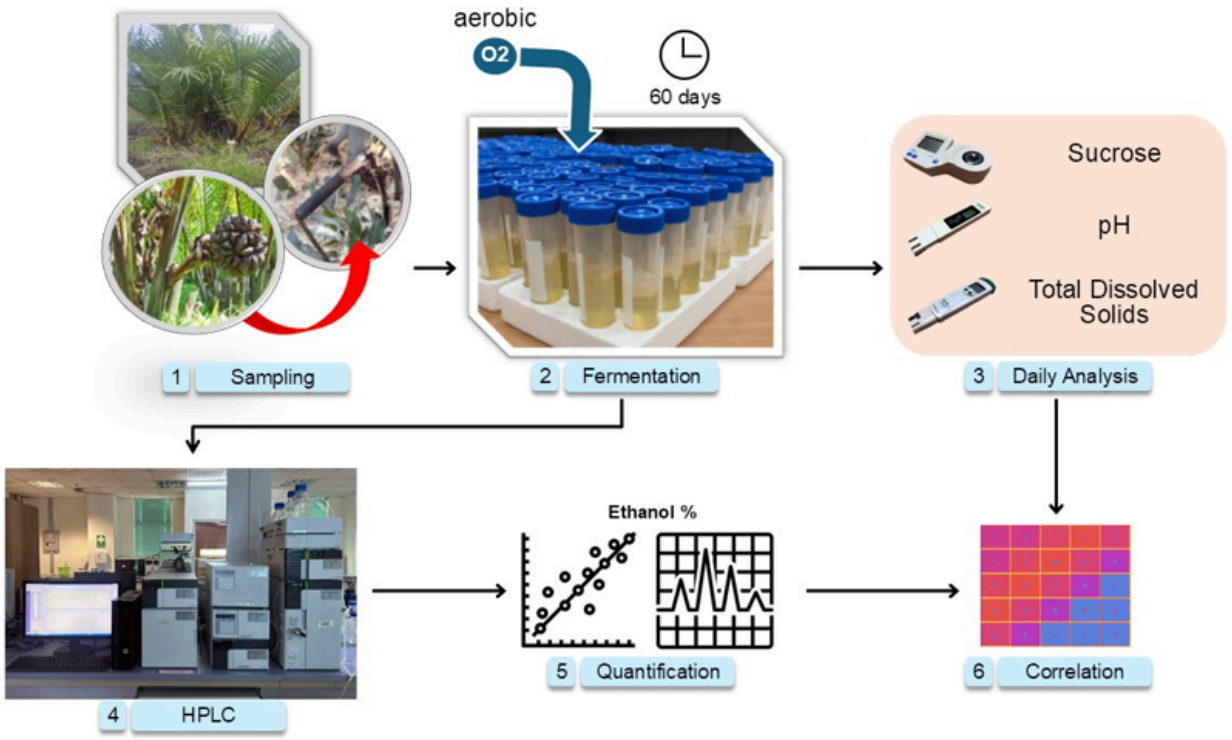


Figure 2

Schematic diagram of the fresh nipa palm sap, fermentation process, quantification and correlation of ethanol.

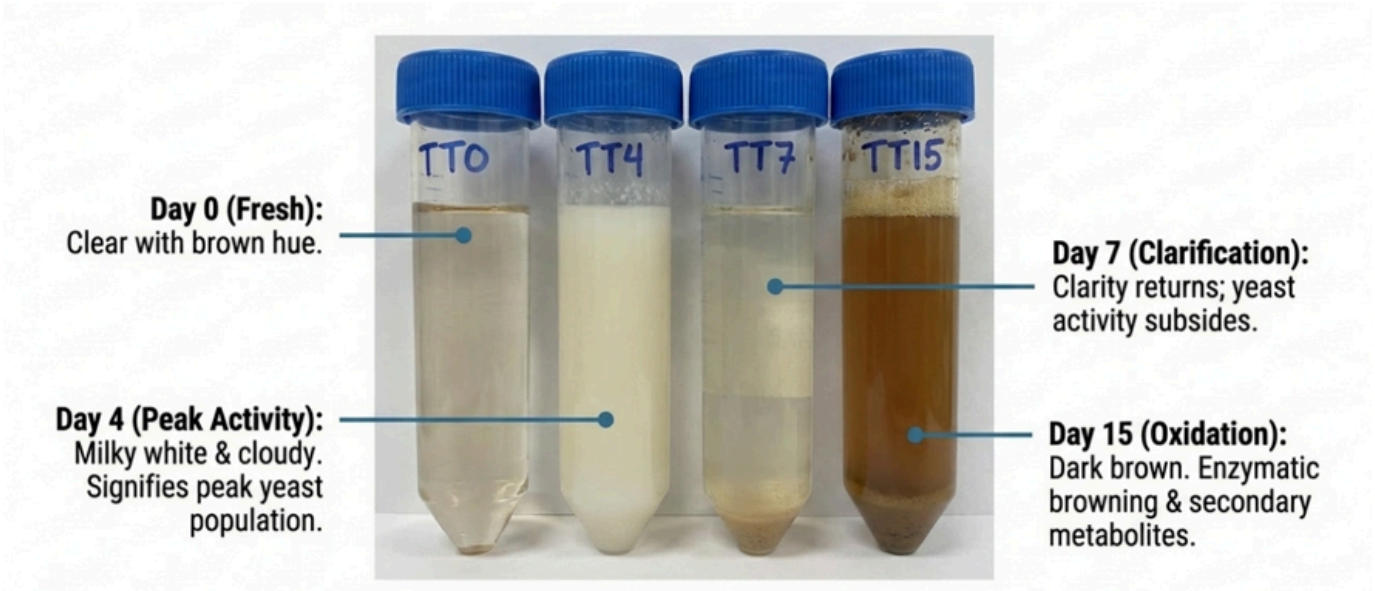


Figure 3

Visual evolution and physical transitions of aerobic fermentation of nipa palm sap at (**a**) Day 0, (**b**) Day 4 with peaked ethanol, (**c**) Day 7 with completed fermentation, (**d**) Day 15 with enzyme oxidation process.

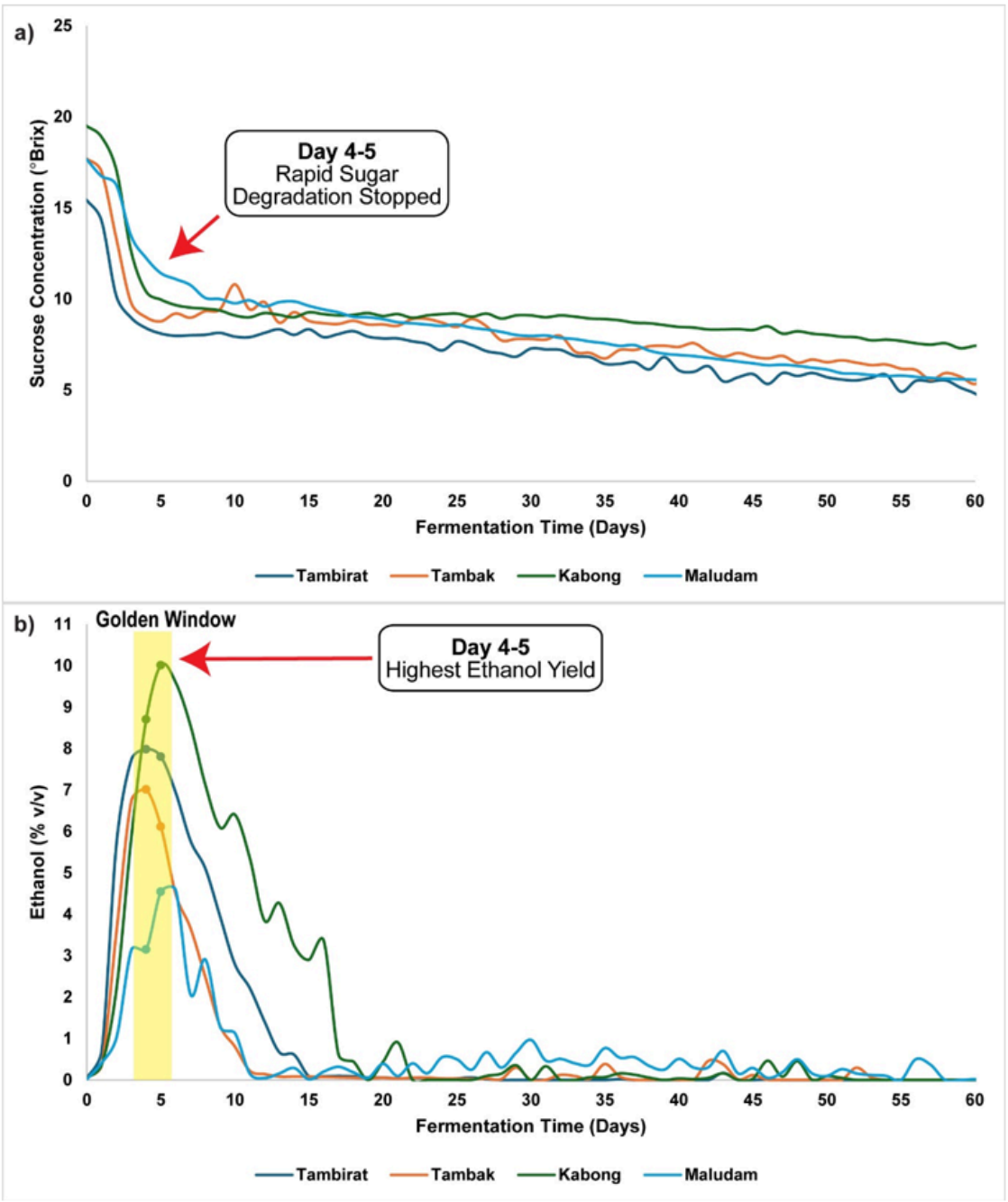


Figure 4

(a) Sucrose (°Brix) and **(b)** ethanol (%v/v) kinetics trend during nipa palm sap fermentation for 60 days. All values are presented as mean ± SD (n=3) and the details are provided in **Supplementary Table S1**.

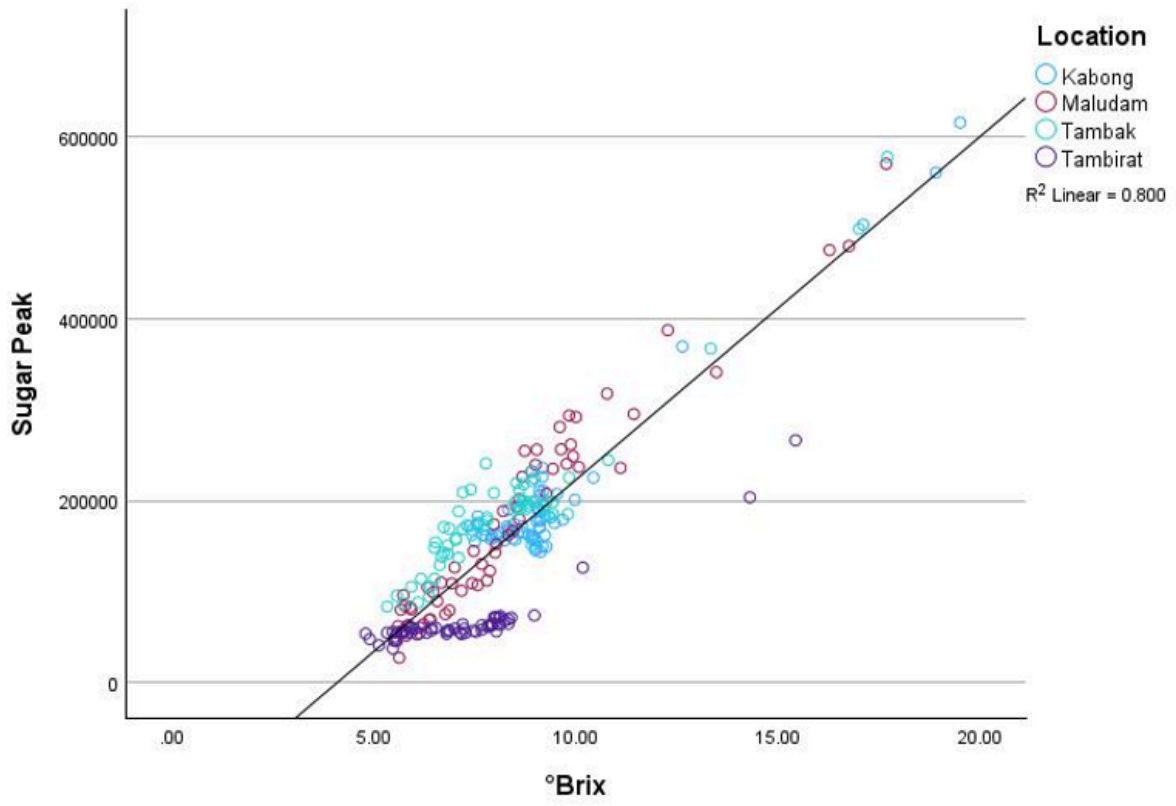


Figure 5

Scatter plot of Sucrose (°Brix) and peak intensities of HPLC on total sugars during 60 days of nipa palm sap fermentation by sampling locations with linearity of R^2 = 0.800.

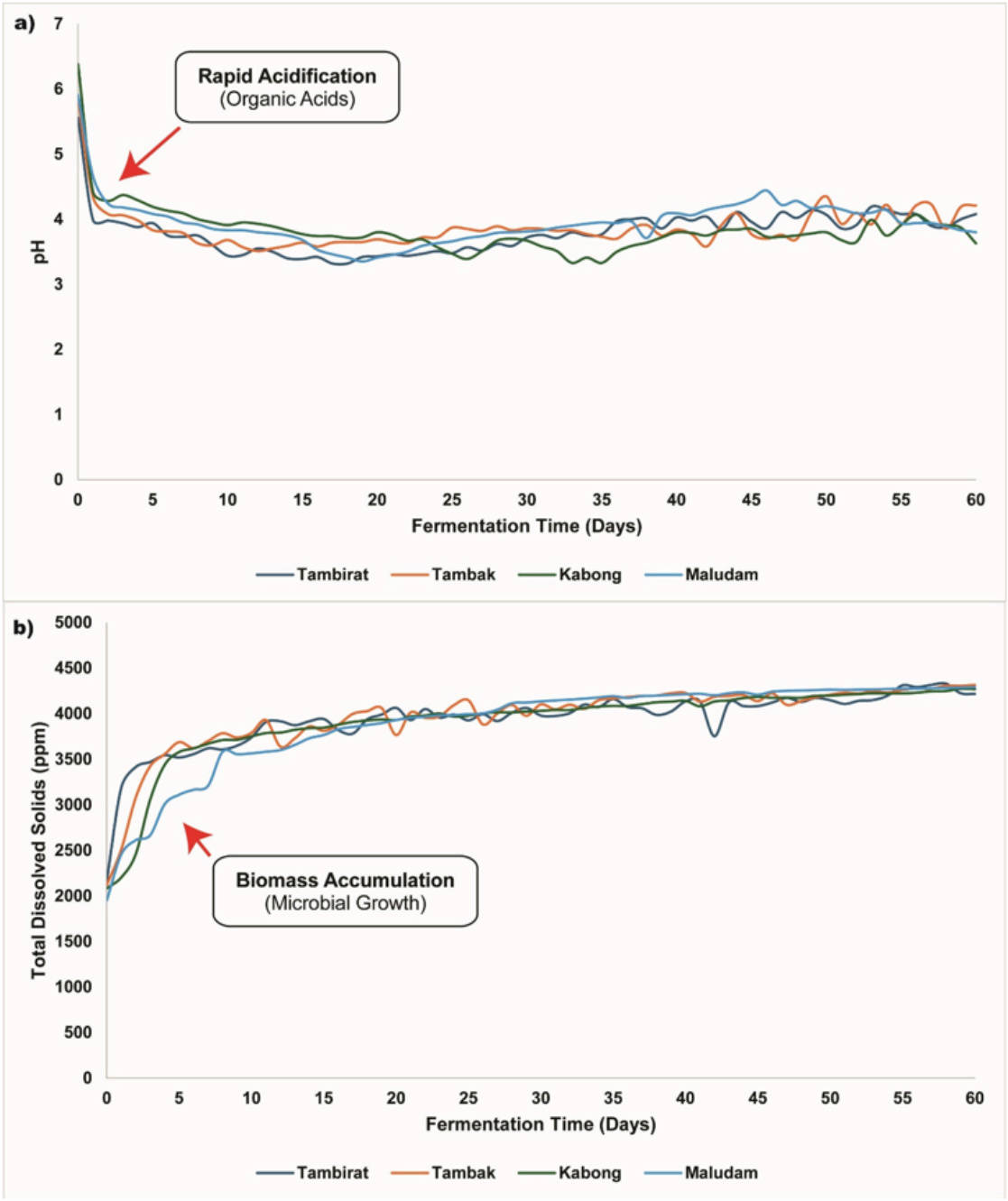


Figure 6

(a) pH and **(b)** TDS dynamics during 60 days of nipa palm sap fermentation with rapid acidification and biomass accumulation. All values are presented as mean ± SD (n=3) and the details are provided in **Supplementary Table S1**.

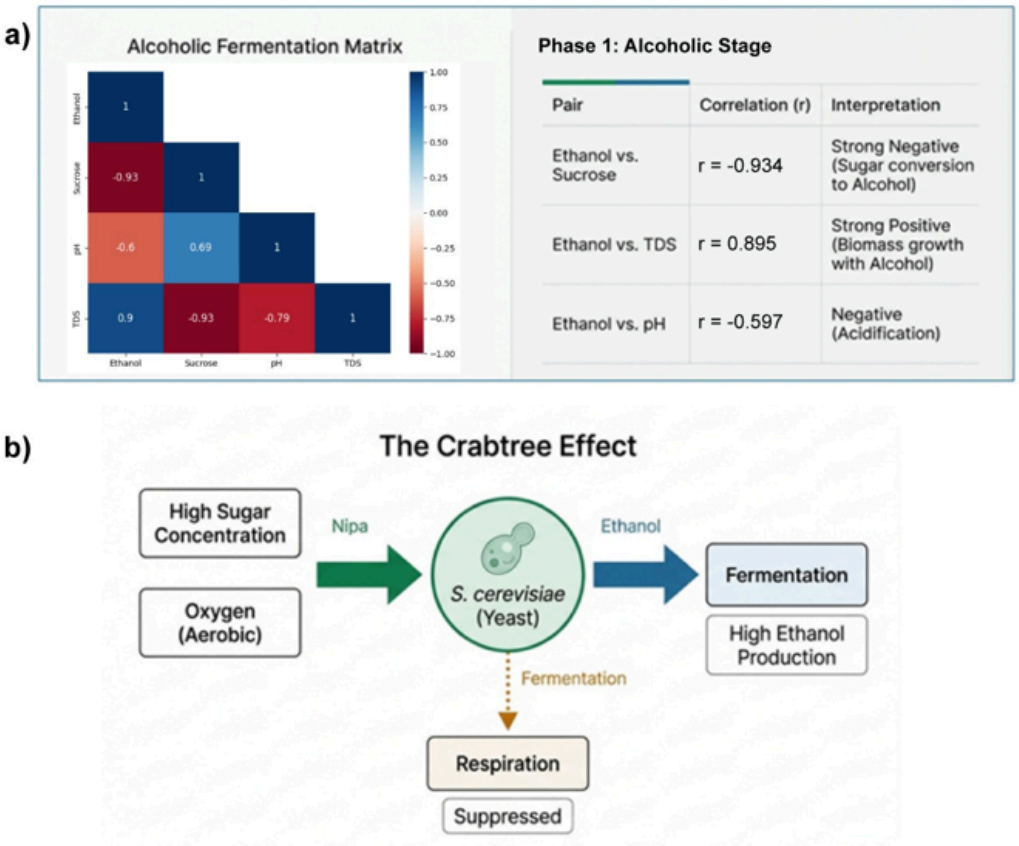


Figure 7

Statistical drivers of the (**a**) alcoholic fermentation phase (Act 1) and **(b)**the Crabtree Effect at the Alcoholic Fermentation Phase (Days 0-4).

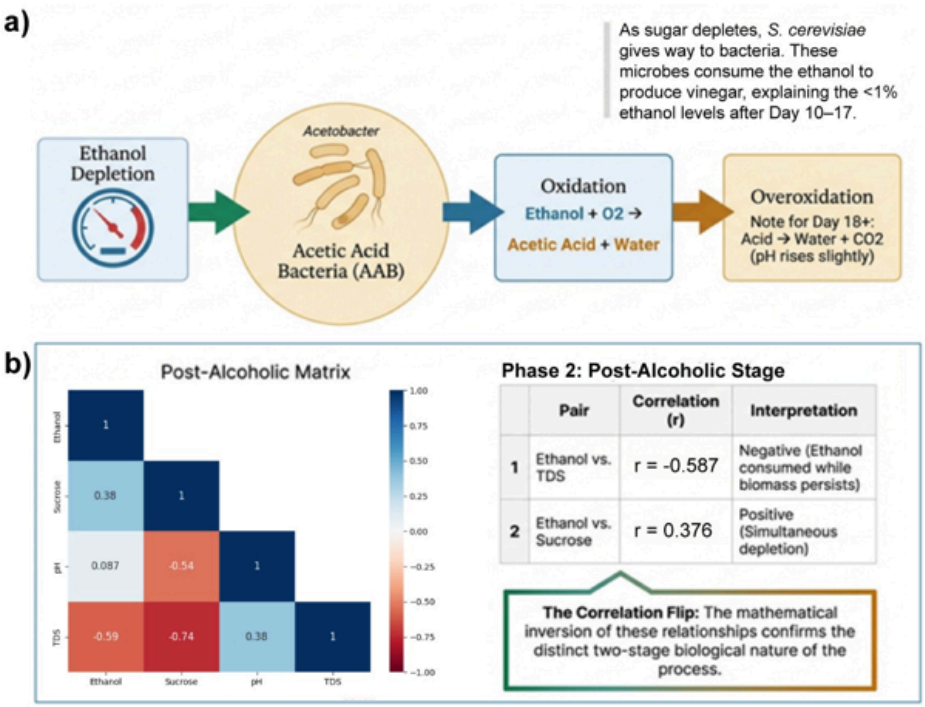


Figure 8

Overoxidation and Post-Alcoholic Phase (Day 5-60) and Statistical drivers of Post-Alcoholic Fermentation Phase.

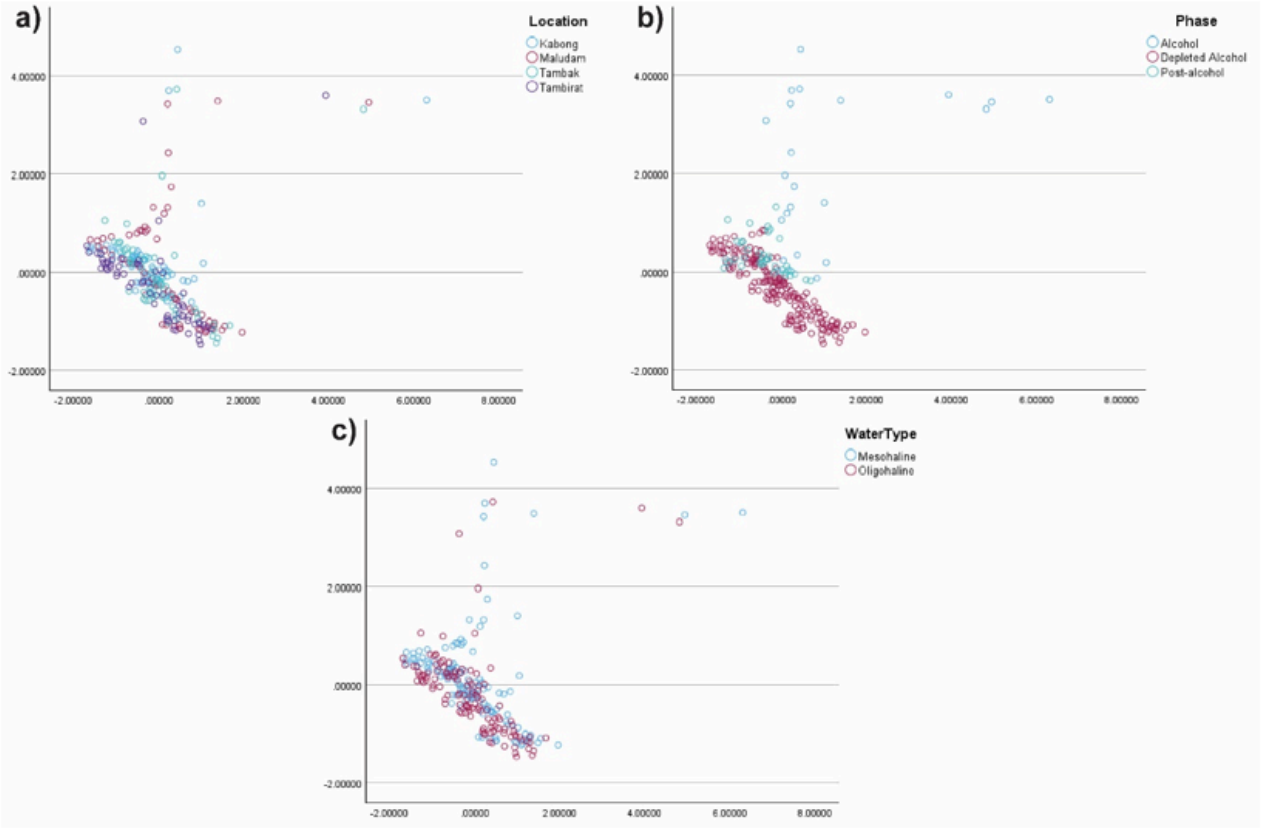


Figure 9

Scatter Plot of the Principal Component Analysis on the Fermentation Trends based on **(a)**Location, **(b)** Phase and **(c)** Water Salinity.

Supplementary Files

This is a list of supplementary files associated with this preprint. Click to download.

- SupplementaryFile.docx
- Scheme1Chemicalreactionduringthetwostagesoffermentation.docx